Mine Water and the Environment (2024) 43:516–528
https://doi.org/10.1007/s10230-024-01004-1

TECHNICAL ARTICLE

Batch Electrocoagulation Process for the Removal of High Colloidal Clay from Open-Cast Coal Mine Water Using Al and Fe Electrodes

Muhammad Sonny Abfertiawan[1] · Mindriany Syafila[1] · Marisa Handajani[1] · Faiz Hasan[1] · Hanifah Oktaviani[1] · Firman Gunawan[2] · dan Febriwiadi Djali[2]

Received: 7 October 2023 / Accepted: 20 August 2024 / Published online: 2 September 2024

Abstract
Open-cast coal mining operations can produce water with high amounts of total suspended solids (TSS). We tested the use of electrocoagulation for the removal of colloidal clay from mine water. Monopolar batch electrocoagulation was performed at the laboratory scale using Al and Fe electrodes and varying the DC current (0.5, 1, and 2 A) and contact time (15, 30, and 45 min). Aluminum electrode electrocoagulation with a current of 2 A and a contact time of 15 min had the greatest TSS removal efficiency (99%), with concentrations decreasing from 5,400 to 23 mg/L. The greatest removal (98 and 99%, respectively) was obtained using an Al electrode with an electric current of 0.5 and 1 A, with 30 min of contact time. With an Fe electrode, the greatest efficiency was achieved with a current of 2 A and a contact time of 30 min. The TSS removal efficiency reached 98% while the concentration dropped to 66 mg/L, followed by 89% and 95% for the 0.5 A-45 min and 1 A-15 min variations, respectively.

Keywords Active treatment · Coagulant · Electrode · Sedimentation

Introduction

In addition to acid mine drainage, coal mines have the potential to produce mine water with high levels of total suspended solids (TSS) (Du et al. 2021; Wang et al. 2021) due to the presence of clay minerals in the overburden. Colloidal clay does not effectively settle (Bergaya et al. 2006; Mohapatra and Kirpalani 2017), which poses a challenge in treating mine water to meet environmental quality discharge standards. Conventional active treatment methods based on chemical processes have been widely developed and used in mining operations (Kleinmann et al. 2022; Trumm 2010; Younger et al. 2002). For mine water with a high TSS, chemical coagulants are used to form flocs, where bonded particles with more mass settle via gravity. With large volumes of mine water, not only are there technical challenges associated with the coagulation method, but the use of chemicals also increases the operational cost of water treatment. Effective and efficient treatment methods have been developed to find and replace these conventional technologies with alternative approaches, such as electrocoagulation, that can effectively and efficiently treat mine water with high TSS concentrations (Dang and Dang 2018; Mollah et al. 2004).

Vik et al. (1984) reported that electrocoagulation was first developed and introduced in England in 1889 to treat domestic wastewater. In 1906, Dietrich patented the principle of electrocoagulation technology for the first time (U.S. Patent 823671) to treat water on ships (Karhu et al. 2012; Rodriguez et al. 2007). Many researchers continue to participate in the development of this technology. In the United States, Harries (1909) developed electrocoagulation to treat wastewater using two electrodes: aluminum (Al) and iron (Fe) (Boinpally et al. 2023; Mao et al. 2023). Electrocoagulation was successfully developed by Matteson et al. (1995) to remove ultrafine particles using Al electrodes. In the electrocoagulation process, the Al electrode causes Al decay at the anode and produces hydroxy ions at the cathode, which react to form aluminum hydroxides. The metal hydroxides function as coagulants (Arnita et al. 2017). Electrodes used

✉ Muhammad Sonny Abfertiawan
msa@itb.ac.id

[1] Water and Wastewater Engineering Research Group, Faculty of Civil and Environmental Engineering, Bandung Institute of Technology, Bandung, Indonesia

[2] Environmental Department, PT. Berau Coal, Berau Regency, Indonesia

in electrocoagulation can be composed of the same or different materials (Emamjomeh and Muttucumaru 2009) and can be monopolar or bipolar (Chen 2004). The electrode materials most commonly used in the electrocoagulation process are iron, aluminum, and titanium (Mollah et al. 2004). Other methods similar to electrocoagulation are known by various names, such as electroflotation, electrooxidation, and electrodecantation (Sillanpaa and Shestakova 2017).

Electrocoagulation can efficiently remove contaminants, producing a colorless, and odorless effluent, with less sludge production than chemical treatment, and the sludge is stable and easily removed (Nur and Effendi 2014). Electrocoagulation has been used with various types of wastewater, such as palm oil industry wastewater with a 90% TSS and 91% chemical oxygen demand (COD) removal efficiency (Amri et al. 2023); paper industry wastewater with 68% COD and 94% color removal (Kumar and Sharma 2022); furniture industry wastewater with 92% COD and 99% TSS removal (Vicente et al. 2023); and textile industry wastewater with the removal of 42% of the TOC, 18% of the COD, 83% of the turbidity, 65% of the TSS, and 90–95% of the color (Bener et al. 2019). In the coal mining industry, electrocoagulation has been shown to reduce metal concentrations from 740 to 0.001 mg/L for 40 min at a current density of 500 A/m^2 (Oncel et al. 2013); the removal of metals (Fe (99%) > Zn (99%) > Mn (99%) > Cu (99%) > Ni (98%) > Cd (96%) > Cr (88%)) (Stylianou et al. 2022); and decreasing sulfate by 54% from 1000 to 460 mg/L (Mamelkina 2017). Solar-powered electrocoagulation has been shown to remove up to 87% of the turbidity (Sharma et al. 2011) and 98% of the chromium in leachate water from landfills (Zaroun and Yari 2019). This approach could increase the opportunity for the use of electrocoagulation in the mining industry, especially in Indonesia, where mines are commonly located in remote areas.

This study focused on removing colloidal clay from mine water. Electrocoagulation could be an alternative treatment technology to address the challenges of treating large volumes of mine water while avoiding the massive use of chemicals in mining areas. The potential use of solar panels is expected to result in low operational costs.

Materials and Methodology

Mine Water Samples

The Sambarata mine site is an active mine owned and operated by PT Berau Coal. The mine, located in the Berau Regency, East Kalimantan, Indonesia has issues with mine water containing high colloidal clay. Rock overburden samples from different lithologies were tested and analyzed using X-ray diffraction (XRD) and X-ray fluorescence (XRF) to determine their mineral compositions. A 100 L sample of mine water was obtained from the Sambarata mine site. Grab sampling was conducted with jerry cans at the inlet of the sediment pond that received run-off water from the mining area. The jerry cans were made of polyethylene and had been cleaned in the laboratory before being taken to the field. Water sampling methods followed the Indonesian National Standard (SNI) 6989.57:2008 Water and Wastewater: Surface Water Sampling Methods.

The mine water samples were dark brown in color (Fig. 1). The characterization of mine water samples, particularly the total metal content, was conducted using inductively coupled plasma mass spectrometry (ICP-MS). Details of the methods used to analyze the mine water characteristics are listed in Table 1. Rock samples from the overburden were obtained and tested for their mineralogy using XRD and XRF at the Hydrogeology and Hydrogeochemistry Laboratory at the Bandung Institute of Technology.

Fig. 1 Sampling sites with high colloidal clay in East Kalimantan coal mine, Indonesia

Table 1 Measurement methods

No	Parameter	Analytical procedure	Standard method
1	pH	pH meter	SNI 6989.11:2019
3	Conductivity	Conductivity meter	SNI 6989.1:2019
4	Temperature	Thermometer	SNI 6989.23:2005
5	TDS	TDS meter	SNI 6989.3:2019
6	TSS	Gravimetric Method	SNI 6989.3:2019
7	Sulfate	Turbidimetry	SNI 6989.20:2019
8	Fe (total)	Atomic Absorption Spectroscopy (AAS)	SNI 6989.84:2019
9	Mn (total)	Atomic Absorption Spectroscopy (AAS)	SNI 6989.84:2019
10	Al (total)	Atomic Absorption Spectroscopy (AAS)	SNI 6989.34:2009
11	43 Other metals	Inductively Coupled Plasma Mass Spectrometry (ICP-MS)	APHA 3125

Electro-coagulation Reactor Design

Laboratory experiments were conducted using an electrocoagulation reactor composed of 5 mm thick acrylic, with a length, width, and height of 14, 10.5, and 20 cm, respectively, and a total capacity of 3 L (Fig. 2). The mine water sample used in the experiment was 1000 mL with two types of electrodes: Al and Fe. Eight monopolar electrodes (four anodes and four cathodes) with a plate thickness of 0.2 cm, a length of 16 cm, and a width of 8 cm were installed. The total depth of the water in the reactor was 7.5 cm, resulting in a total anode wet surface area of 0.024 m^2. The electrodes were mounted using a distance of 1.5 cm between the plates. All the electrodes were connected to an electric current from a DC current source (MDB 0–60 V and 0–20 A). The current and voltage measurements were performed using a MASDA DT830B multimeter.

Treatment Procedure

As much as 1 L of mine water with colloidal clay content was put into the reactor. Three current variations (0.5, 1, and 2 A) and three contact time variations (15, 30, and 45 min) were tested. After the contact time, the DC power supply was turned off, and the mine water was allowed to settle. The sedimentation process to separate the solid particles in water was carried out for 60 min in all experiments. Then the supernatant (the clear liquid over the sediment) was sampled at 3 cm from the water surface (halfway between the water surface and the bottom of the reactor) to analyze its characteristics.

The electrocoagulation process (Fig. 3) was carried out nine times in duplicate for a total of 18 experiments. Electrocoagulation was conducted in the laboratory with an average room temperature of 25 °C. Water quality parameters were tested after treatment using the Standard National Indonesia (SNI) procedure.

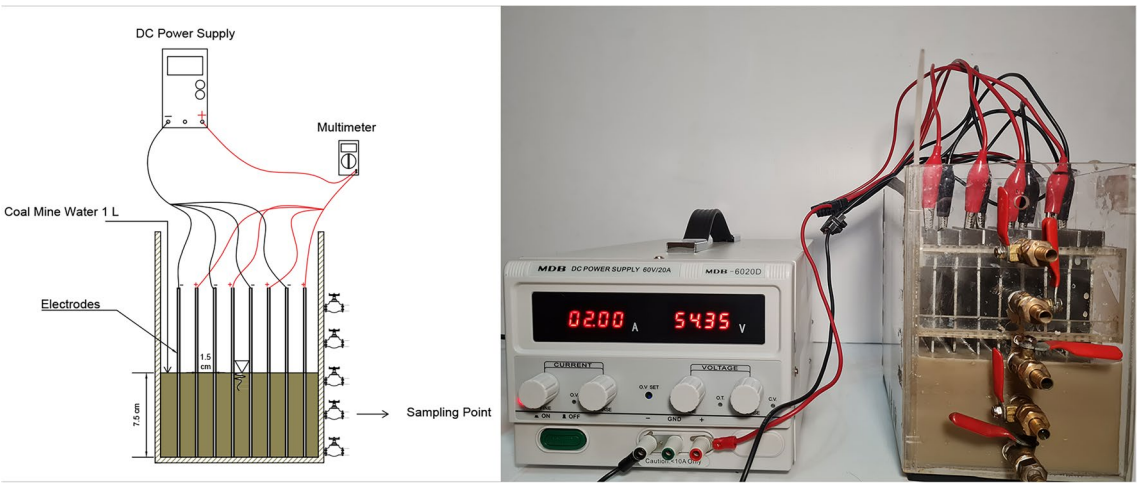

Fig. 2 Design and schematic of the electrocoagulation reactor (*batch*)

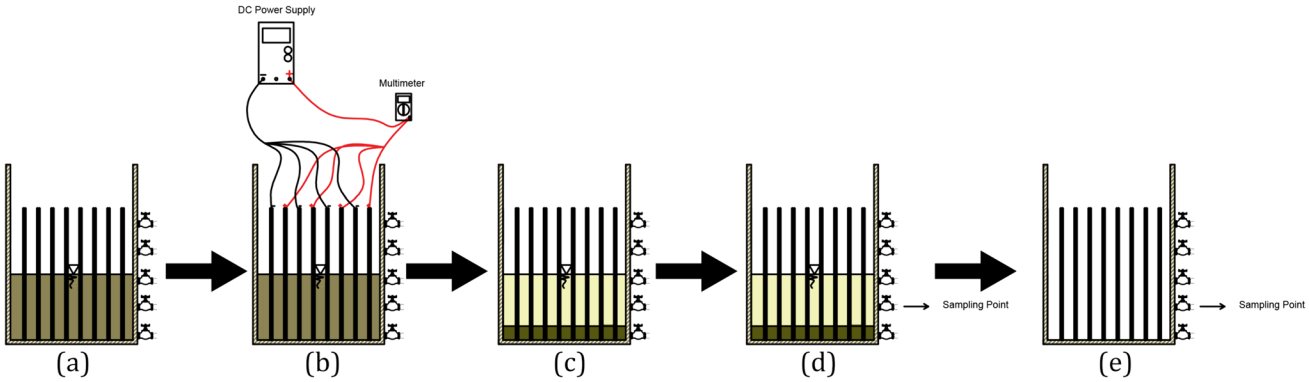

Fig. 3 The steps of batch electrocoagulation experiments: **a** mine water is filled as much as one liter into the reactor, **b** electrodes in the reactor are electrified with direct current (DC), **c** mine water is allowed to settle for 60 min, **d** mine water is sampled at the midpoint of the reactor, and **e** the reactor is ready to be reused for other variations

Results and Discussion

Characteristics of the Mine Water Samples

The water samples from the Sambarata mine site contained high amounts of colloidal clay with TSS concentrations of 5400 mg/L. Mineralogical tests on the two overburden samples showed clay minerals, including the vermiculite and illite mineral groups. Vermiculite does not form through crystallization from solution, but through alteration or selective replacement of ions in the clay structure without damaging the structure. Vermiculite and montmorillonite contain highly hydrated exchangeable cations, mainly Ca and Mg, in the interlayer (Abollino et al. 2008; Dos Anjos et al. 2014), with a large surface area per unit mass and fine particle size.

Another group of clay minerals detected in the mineralogical tests was illite, also known as "clay micas," which have the general formula of $KyAl_4(Si8\text{-}y, Aly)O_{20}(OH)_4$. This mineral has a layered structure and is a swelling and dispersible clay (Hamza et al. 2023). However, illite swells less than montmorillonite due to its different charge densities and interlayer cation types (Chen et al. 2020). Montmorillonite can host a range of different interlayer cations including Ca^{2+}, Na^{+}, Mg^{2+}, K^{+}, and Sr^{2+}, whereas illite only has K^{+} (Kahr and Madsen 1995; Marsh et al. 2018). Therefore, illite can have markedly less cation exchange capacity than montmorillonite. In soils influenced by high rainfall, illite minerals transform into montmorillonite, whereas, under the influence of temperate or high-temperature climates, illite structures can transform into kaolinite structures. The full results of the mineralogical characterization are presented in Tables 2 and 3.

Clay minerals have the potential to interact with metal cations often contained in wastewater, including adsorption by ion exchange, precipitation as hydroxides or oxide hydrates on clay surfaces, and adsorption as complex species (Lagaly 2006; Węgrzyn et al. 2022). Thus, colloidal particles can also interact with metals and carry them over long distances (Cao et al. 2022; Chen et al. 2018). Table 4 presents the characteristics of the mine water samples sourced from overburdened areas containing clay minerals. The mine water had a TSS concentration of 5,400 mg/L. Several metals were present at relatively high concentrations, including total iron Fe (52 mg/L), total Al (26.63 mg/L), Na (127.9 mg/L), K (11.9 mg/L), Ca (7.4 mg/L), and Mg (4.6 mg/L). The metal content in the mine water is consistent with the characteristics of the rock samples obtained from the XRF test results.

The Effect of pH

The pH of the solution contributes to the solubility of metal hydroxides, which can affect the electrocoagulation efficiency. Changes in the pH (Fig. 4) occurred throughout the electrocoagulation experiment. The experimental results show that mine water treated using Al and Fe electrodes experienced an increase in pH, as mentioned by Mouedhen et al. (2008). The Fe electrodes produced a higher pH (10–11) than the Al electrodes (a pH of 9–11). The increase in pH is due to the accumulation of hydroxide ions (OH^{-}) during electrocoagulation (Ni'am et al. 2007; Syaichurrozi et al. 2020). The pH increased with greater current and contact times. Additionally, dissolved carbonate changes the pH because CO_2 forms during electrocoagulation when H_2 microbubbles form at the cathode (Weiss et al. 2021). In this study, an increase in the pH > 9 had the potential to exceed the environmental quality discharge standards (pH values of 6–9).

Table 2 X-ray diffraction (XRD) test results

Phase name	Formula	Figure of merit	Content (%)	Mineral TYPE
Sample #1				
Quartz	SiO_2	0.95	49(17)	Main (Felsic)
Vermiculite	$(Mg_{2.36}\ Fe_{48}\ Al_{16}\ Al_{1.28}\ Si_{2.72})\ O_{10}\ (OH)_2\ (H_2O)_6\ Mg$	1.2	0.83(13)	Clay
Muscovite	$KAl_3Si_3O_{10}(OH)_2$	1.6	37(5)	Main (Felsic)
Titanomagnetite	Fe_2TiO_4	1.5	2.2(14)	Magnetic
Pyroxene	$CaMgSi_2O_6$	1.8	0.8(7)	Main (Mafic)
Albite	$Na(AlSi_3O_8)$	1.5	1.8(6)	Na-Plagioclase
Posnjakite	$Cu_4(SO_4)(OH)_6\ (H_2O)$	1.2	8.1(10)	Sulfide
Sample #2				
Augite	$(Ca_{818}\ Mg_{792}\ Fe_{183}\ Fe_{.086}\ Al_{151}\ Al_{269}\ Si_{1.751})\ O_6$	1.4	2.5(8)	Main (Mafic)
Hollandite	$K_{1.54}\ Ti_{7.23}\ Mg_{0.77}\ O_{16}$	1.7	17(9)	Oxides
Todorokite	$NaMn_6O_{12}\ 3H_2O$	1.4	6.6(7)	Manganese (metals)
Vermiculite	$Mg_{3.41}Si_{2.86}\ Al_{1.14}\ O_{10}\ (OH)_2$ (H2 O)3.72	1.4	0.54(7)	Clay
Quartz	SiO_2	0.33	66(5)	Main (Felsic)
Illite-2M#2	$KAl_2(Si_3Al)O_{10}(OH)$	1.1	1.4(6)	Clay (Main-Ilit)
Muscovite 2M1—from Effingham township, Ontario, Canada	$KAl_2(AlSi_3O_{10})(OH)_2$	1.5	3.5(8)	Main (Felsic)
Microcline	$KAlSi_3O_8$	1.7	0.15(14)	Alkali Feldspar (Felsic)
Pyroxene	$Mg_2Si_2O_6$	1.8	1.3(5)	Main (Mafic)

Table 3 X-ray fluorescence (XRF) test results

Sample #1				Sample #2			
No	Component	Result mass %	Intensity	No	Component	Result mass %	Intensity
1	Na	0.098	0.015	1	Na	0.015	0.0084
2	Mg	0.63	0.25	2	Mg	0.48	0.19
3	Al	17	27	3	Al	18	30
4	Si	61	57	4	Si	64	57
5	P	0.061	0.033	5	P	0.033	0.017
6	Si	1	1	6	S	0.95	0.90
7	Cl	0.023	0.035	7	Cl	0.017	0.024
8	K	5.5	3.8	8	K	5.8	3.7
9	Ca	0.95	0.97	9	Ca	0.32	0.30
10	Ti	1.8	0.55	10	Ti	2.3	0.64
11	Mn	0.12	0.12	11	Mn	0.083	0.083
12	Fe	10.9	18	12	Fe	7.5	12
13	Ni	0.038	0.093	13	Zn	0.060	0.25
14	Cu	0.030	0.091	14	Rb	0.053	0.61
15	Zn	0.039	0.16	15	Sr	0.024	0.31
16	Rb	0.052	0.57	16	Zr	0.096	1.7
17	Sr	0.047	0.58				
18	Y	0.0052	0.38				
19	Zr	0.084	1.5				

The Effect of Total Dissolved Solids (TDS)

The raw mine water sample had a total dissolved solids (TDS) concentration of 320 mg/L. The TDS in wastewater can result from dissolved organic matter and inorganic salts, including sodium, potassium, calcium, magnesium, chloride, bicarbonate, and sulfate (Chen et al. 2021). APHA (2017) defines TDS as the constituents of total solids in a water

Table 4 Characteristics of the raw mine water

No	Parameters	Unit	Value	No	parameters	Unit	Value
1	pH	–	8	28	Se	mg/L	0.0059
2	Conductivity	µS/cm	540	29	Rb	mg/L	0.0050
3	Temperature	°C	26	30	Sr	mg/L	0.088
4	TDS	mg/L	320	31	Y	mg/L	0.0012
5	TSS	mg/L	5,400	32	Mo (97)	mg/L	0.0016
6	Sulfate	mg/L	49	33	Mo (98)	mg/L	0.0016
7	Fe (total)	mg/L	52	34	Ag	mg/L	< 0.0000001
8	Mn (total)	mg/L	0.33	35	Cd	mg/L	< 0.0000001
9	Al (total)	mg/L	27	36	Cd	mg/L	< 0.0000001
10	Fe (dissolved)	mg/L	1.3	37	Te	mg/L	0.000041
11	Mn (dissolved)	mg/L	0.0039	38	Ba	mg/L	0.030
12	Al (dissolved)	mg/L	0.31	39	La	mg/L	0.0019
13	Li	mg/L	< 0.0000001	40	Ce	mg/L	0.0043
14	Be	mg/L	0.00046	41	Pr	mg/L	0.00065
15	B	mg/L	0.051	42	Nd	mg/L	0.0025
16	Na	mg/L	130	43	Sm	mg/L	0.00037
17	Mg	mg/L	4.6	44	Eu	mg/L	0.00011
18	K	mg/L	12	45	Gd	mg/L	0.00037
19	Ca	mg/L	7.4	46	Dy	mg/L	0.00030
20	V	mg/L	0.0027	47	Ho	mg/L	0.000059
21	Cr	mg/L	0.0015	48	Er	mg/L	0.00012
22	Co	mg/L	0.00041	49	Tm	mg/L	0.000017
23	Ni	mg/L	0.0027	50	Yb	mg/L	0.00011
24	Cu	mg/L	0.011	51	TI	mg/L	< 0.0000001
25	Zn	mg/L	0.0071	52	Pb (206)	mg/L	0.00027
26	Ga	mg/L	0.00033	53	Pb (207)	mg/L	0.000022
27	As	mg/L	0.0041	54	Pb (208)	mg/L	0.000078
				55	U	mg/L	0.00047

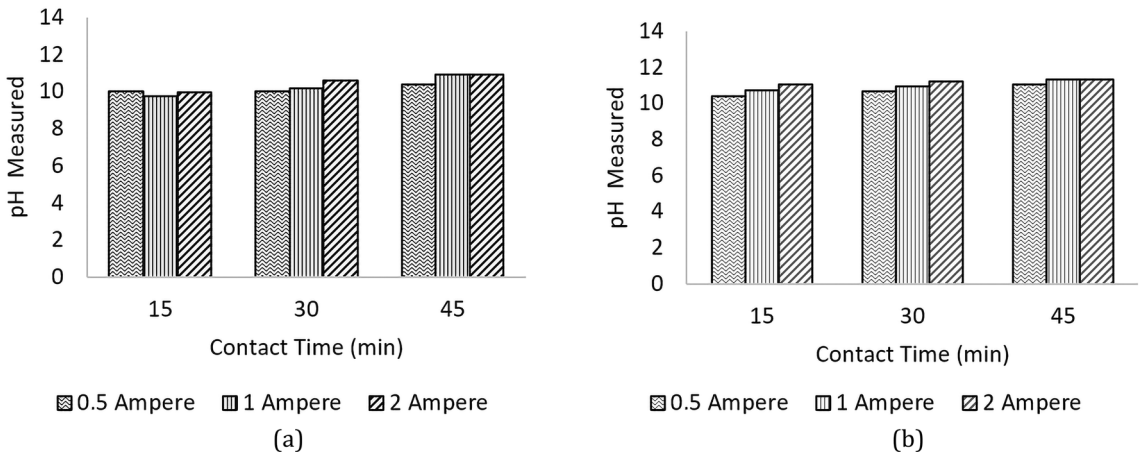

Fig. 4 Effect of current on pH changes: **a** aluminum electrodes and **b** iron electrodes

sample that pass through a nominal pore size of 2.0 µm or less under specified conditions.

The TDS concentration changed with both the Al and Fe electrodes, increasing with the magnitude of current and contact time (Fig. 5). The electrocoagulation process using Fe electrodes caused a greater increase in the TDS concentration than the Al electrodes. At a current variation of 2 A and a contact time of 30 min, the TDS value for

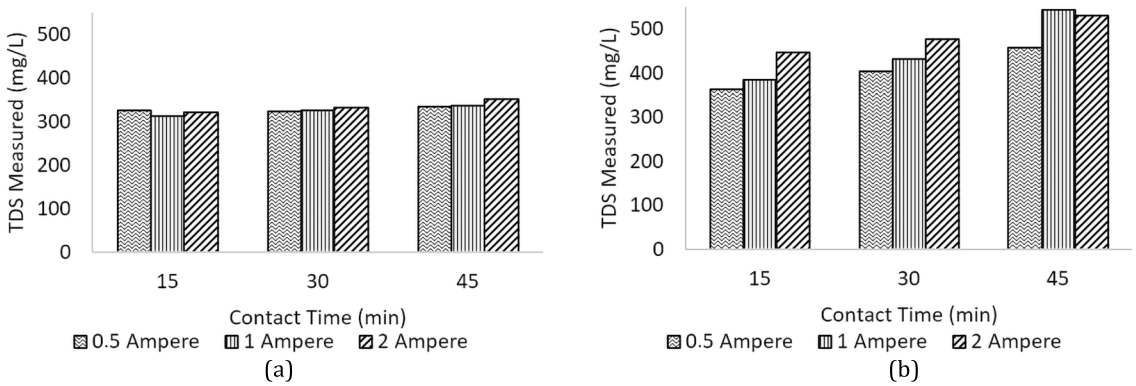

Fig. 5 Measured TDS (mg/L) after a 60-min settling time: **a** aluminum electrodes and **b** iron electrodes

the Al electrode reached 332 mg/L while that for the Fe electrode was 447 mg/L. The Al^{3+} and Fe^{2+} ions generated from the electrodes acted as charge neutralization agents for the negative ions in the pollutant particles. The presence of these ions decreased the electrical double layer, thus allowing coagulation. This can be attributed to the high concentration of sodium (Na) relative to other cations in the raw samples. The introduction of Al^{3+} and Fe^{2+} can exchange Na and decrease the electrical double layer. However, most of the Al^{3+} and Fe^{2+} can be lost as insoluble hydroxides at neutral and alkaline pH, thereby limiting the availability of cations for ion exchange. Therefore, sweep flocculation and hetero-coagulation are considered the primary factors that control coagulation in this system (Duan and Gregory 2003; Ghernaout and Ghernaout 2012). The release of Al^{3+} and Fe^{2+} ions from the electrode plate (anode) formed $Al(OH)_3$ and $Fe(OH)_2$ flocs, which could bind to contaminants and particles in the wastewater (Harahap et al. 2024). The main reactions occurring on the Fe electrodes were as follows:

$$\text{Anode}: \ Fe_{(s)} \rightarrow Fe^{2+}_{(aq)} + 2e^{-}$$

$$Fe^{2+}_{(aq)} + 2OH^{-}_{(aq)} \rightarrow Fe(OH)_{2(s)}$$

$$\text{Cathode}: \ 2H_2O_{(l)} + 2e^{-} \rightarrow H_{2(g)} + 2OH^{-}_{(aq)}$$

$$\text{Overall}: \ Fe_{(s)} + 2H_2O_{(l)} \rightarrow Fe(OH)_{2(s)} + H_{2(g)}$$

The reaction that occurred on the Al electrodes was as follows:

$$\text{Anode}: \ Al_{(s)} \rightarrow Al^{3+}_{(aq)} + 3e^{-}$$

$$\text{Cathode}: \ 3H_2O_{(l)} + 3e^{-} \rightarrow 3/2\, H_{2(g)} + 3OH^{-}_{(aq)}$$

$$\text{Overall}: \ Al^{+3}_{(aq)} + 3H_2O_{(l)} \rightarrow Al(OH)_{3(s)} + 3H^{+}_{(aq)}$$

Additionally, the formation of metal hydroxide precipitates used in the sweep coagulation process also plays a role in increasing the TDS levels in wastewater. At higher current densities and contact times, there was an increase in ions with different charges on the dissolved particles in wastewater, which resulted in the formation of flocs that then agglomerated into larger flocs (Nur and Effendi 2014).

The Effect of Temperature

The increase in temperature was directly proportional to the contact time and current during the experiment using the Al and Fe electrodes (Fig. 6). With a current variation of 2 A and a contact time of 30 min, the Al electrode produced a higher temperature than the Fe electrode. The temperature at the Al electrode reached 49.5 °C and the Fe electrode was 31.5 °C. Increased temperatures promote the formation of metal hydroxides and lead to greater particle collisions and mobility (El-Ashtoukhy et al. 2009). The formation of metal hydroxides during the electrocoagulation process triggers the release of heat, which increases the reaction rate (Holt 2002). The temperature changed linearly with the contact time, current, and electrolyte concentration. Additionally, higher temperatures allow for the formation of larger hydrogen bubbles, which can increase flotation speed (Koren and Syversen 1995). The increase in temperature during the electrocoagulation process was due to the release of Al^{3+} and Fe^{2+} ions. The greater the current and time applied to the system, the greater the collision between particles due to the release of metal hydroxides in the system.

Total Suspended Solids and Metal Concentrations

The changes in the TSS concentrations during the electrocoagulation process are shown in Fig. 7. The experimental results show that in the smallest variable scenario, i.e. a current of 0.5 A and a contact time of 15 min, the TSS concentration was still relatively high with the Al electrode (341 mg/L) and 2113 mg/L for the Fe electrode. This

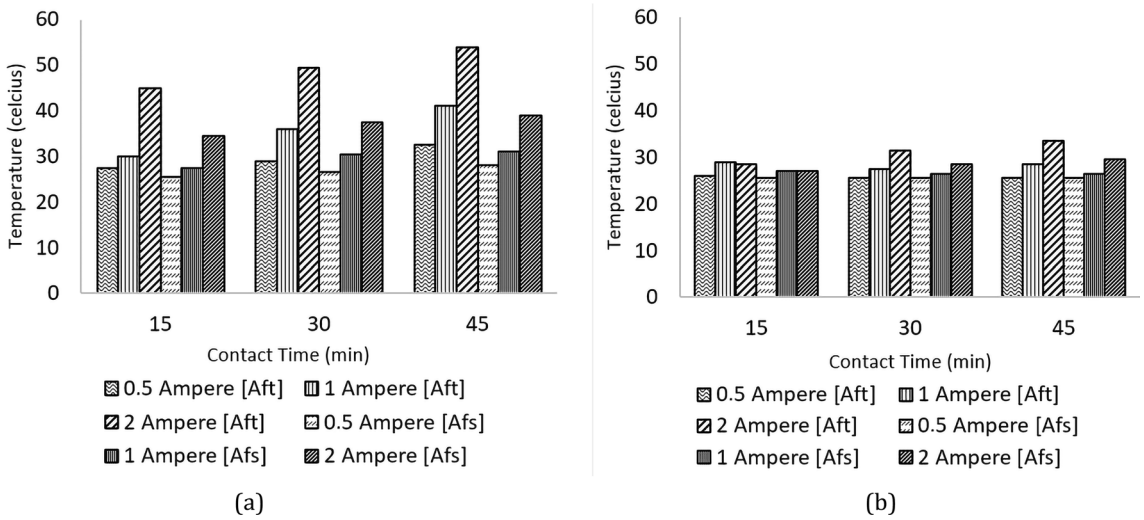

Fig. 6 Average measured temperature after treatment time [Aft] and after a 60-min settling time [Afs]: **a** aluminum electrodes and **b** iron electrodes

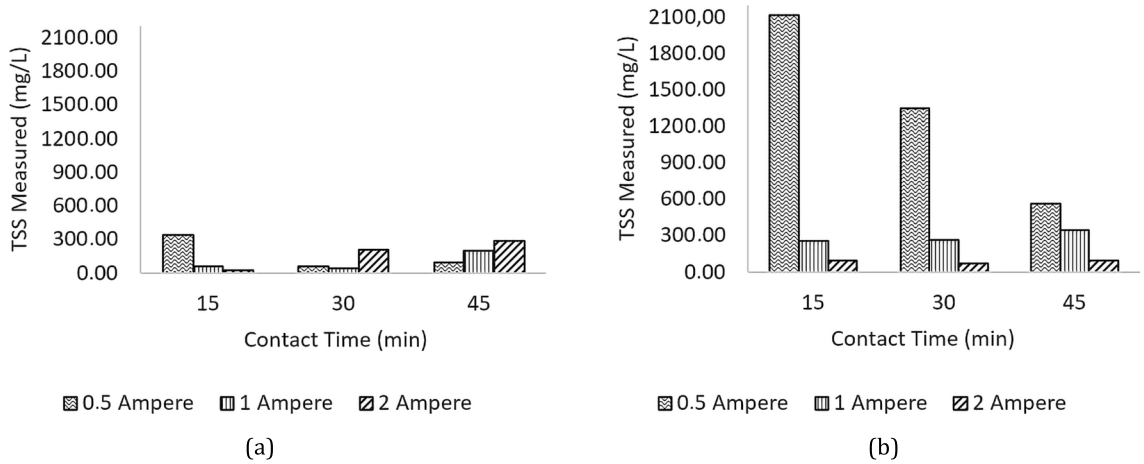

Fig. 7 Measured TSS (mg/L) after a 60 min settling time: **a** aluminum electrodes and **b** iron electrodes

occurred owing to the formation of metal hydroxides, which function as coagulants; this was not sufficient to bind solid particles in the mine water. The 2 A current and contact time of 15 min at the Al electrode achieved the highest TSS removal of 99% from an initial concentration of 5400 to 23 mg/L. The Fe electrodes yielded different results, achieving the greatest efficiency at 2 A and a contact time of 30 min with a TSS removal of 98% from the initial concentration of 5400 to 66 mg/L. The solubility of metal hydroxide precipitates is an important factor in TSS removal and is largely determined by pH. At lower pH values from (3.3 to 10), the solubility of metal hydroxide precipitates produces positive charges, Al^{3+}; $Al(OH)_{3(s)}$ was the dominant Al species. At pH values > 10, negatively charged $Al(OH)^{4-}$ forms (Linares-Hernández et al. 2009). This is consistent with Hudori (2008), who found that the best level of pollutant removal in electrocoagulation using Al electrodes occurred in the pH range of 4–10 due to the formation of a coagulant ($Al(OH)_3$).

The TSS concentration also has the potential to increase due to excessive bubble production at the cathode. Theoretically, bubbles in the electrolyte solution of a sample have a stirring function owing to the upward momentum. With enough bubbles, there may be an increase in the contact between the coagulant and solid particles. However, excessive bubbling can cause poor floc formation, preventing particles from agglomerating. Operation at small currents produces relatively few bubbles, causing slow stirring and incorrect flocculation. If the current density increases, the production of bubbles increases and the upward momentum

movement accelerates, which increases the mixing. The shear force from excessive mixing can damage and break up the flocs, reducing the effectiveness of pollutant removal.

The dissolution of the Al electrode initially produced monomer cations, such as Al^{3+}, which changed into $Al(OH)_3$ at appropriate pH values and eventually polymerized into Al complexes ($Al_n(OH)_{3n}$). Aluminum complexes, such as $Al(OH)^{2+}$, $Al_2(OH)_2^{4+}$, and $Al(OH)_4^-$, can form depending on the pH of the solution (Mollah et al. 2001). In this study, the results showed that variations using Al electrodes produced pH values of up to 10.9. At this pH, the dominant Al complex was soluble $Al(OH)^{4-}$. This is consistent with the results in Table 5, which indicate that the dissolved Al concentration in the effluent water increased with the variation in the Al electrodes. Although the experiments with Fe electrodes produced a greater pH than the Al electrodes (up to 11), highly insoluble compounds ($Fe(OH)_{2(s)}$) form predominantly at pH values > 7.5 (Linares-Hernández et al. 2009). Therefore, Table 5 indicates that the dissolved Fe in the solution tended to show a small concentration variation using Fe electrodes. Metal removal is also possible due to the presence of a gelatinous suspension ($Al(OH)_3$ and $Fe(OH)_n$) via adsorption, which produces charge neutralization and enmeshment in the precipitate (Mollah et al. 2001).

The final level of total suspended solids (TSS) in this experiment, with the greatest variation of removal, was 22.84 mg/L. These results meet the applicable quality standards set by the government (Table 6): the TSS, Fe, and manganese values were appropriate, but the pH value exceeded the standard. Therefore, further study is needed, focusing on the pH value.

Table 5 Dissolved metal concentrations of the effluent at the aluminum and iron electrodes (greatest efficiency variation) using ICP-MS

No	Elements	Unit	Raw mine water	Aluminum electrodes (2 A and 15 min)	Iron electrodes (2 A and 30 min)
1	Be	mg/L	0.00046	0.00081	0
2	B	mg/L	0.049	0.072	0.38
3	Na	mg/L	130	140	141
4	Mg	mg/L	4.6	0.014	0.33
5	Al	mg/L	0.31	8.1	0.47
6	K	mg/L	12	13	9.2
7	Ca	mg/L	7.4	0.18	1.1
8	V	mg/L	0.0027	0.0023	0.00096
9	Cr	mg/L	0.0015	0	0.019
10	Mn	mg/L	0.0039	0	0.013
11	Fe	mg/L	1.3	0.022	0.64
12	Co	mg/L	0.00041	0.00006	0.0014
13	Ni	mg/L	0.0027	0.00019	0.055
14	Cu	mg/L	0.011	0.00092	0.0034
15	Zn	mg/L	0.0071	0.0041	0.018
16	Ga	mg/L	0.00033	0.0087	0.00031
17	As	mg/L	0.0041	0.0052	0.00041

The Effect of Electrode Material: Al vs Fe

The type of electrode used in electrocoagulation has a major effect on the amount and type of metal ions contained in the solution, coagulant efficiency, and cost (Ebba et al. 2021; Moneer et al. 2023; Sadik 2019; Tiaiba et al. 2017). The electrode type affects the voltage generated during the electrocoagulation process according to the reactivity series of the metals. In Fig. 8, the more that the metal is to the left of its position in the reactivity series of metals, the more reactive the metal is, or the easier it is to release electrons (i.e. a strong reductant) and is easily oxidized. Meanwhile, the more to the right, the less reactive the metal or the more difficult it is to release electrons and the stronger the oxidizer (i.e. more easily reduced; Dogra and Dogra 1990). Iron metal is located to the right of Al metal, such that the Fe electrode is less reactive; therefore, the metal ions produced are less reactive than the Al electrode.

After 18 experiments, changes in the shapes of the Al and Fe electrodes were observed (Fig. S-1). The surface of the

Table 6 Comparison of batch electrocoagulation results and discharge requirements

No	Parameter	Unit	Aluminum electrodes (2 A and 15 min)	Iron electrodes (2 A and 30 min)	Discharge requirements
1	TSS	mg/L	23	66	300[a]
2	Dissolved iron (Fe)	mg/L	0.02	0.64	0.3[b]
3	Dissolved manganese (Mn)	mg/L	0	0.013	0.4[b]
4	pH	mg/L	9.9	11	6.0–9.0[a]

[a]East Kalimantan Provincial Regulation No 02 of 2011 Water Quality Management and Water Pollution Control

[b]Government Regulation of the Republic of Indonesia No 22 of 2021 Implementation of Environmental Protection and Management (Appendix VI)

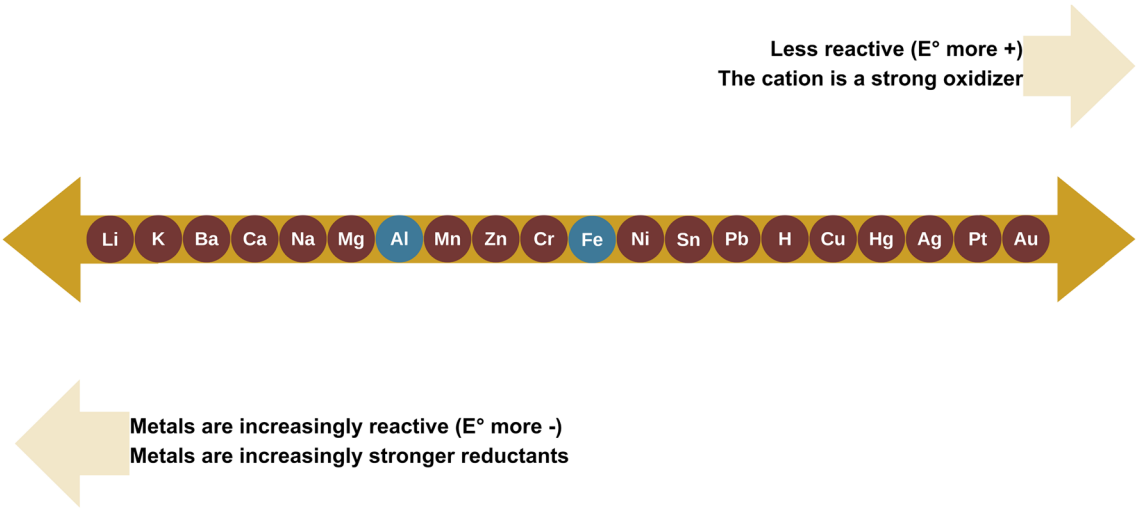

Fig. 8 Reactivity series of metals

anode exhibited small holes due to corrosion. The anode, often referred to as the "sacrificial electrode," experienced corrosion with the removal of the coagulant agent into the solution. The greater the current, the faster the corrosion of the anode plate, due to the faster ion release rate. This statement supports one of the drawbacks of electrocoagulation technology: the anode must be replaced periodically (Mollah et al. 2004). No corrosion pits were detected on the cathode plates. This is because the cathode is inert. However, on the cathode plate, white spots indicated the release of hydrogen ions in that section (Nur and Effendi 2014). Related to this, Syafila et al. (2023) discussed electrode selection using a statistical approach.

The Effect of Current and Contact Time

In this study, Fe and Al electrodes were used at a distance of 1.5 cm. The smaller the distance between the electrodes, the less voltage was required. The Fe and Al electrodes produced different voltages at the same current and contact time. At the same current strength of 2 A with a contact time of 30 min, the Al electrode produced a voltage of 46 V, while the Fe electrode produced 11 V (Fig. S-2).

The amount of current and contact time determined coagulant production. An optimal combination was required to achieve the highest TSS removal rate. Current density determines the coagulant dosage, floc production rate, and size of the bubbles released from the electrode process (Hidayanti et al. 2021). Current and time variations that are smaller than the optimal conditions cannot remove TSS owing to the lack of coagulant produced, whereas larger and excessively fast currents and times can break the flocs that have been formed due to too much hydrogen bubble production, reducing the effectiveness of pollutant removal (Setyawati et al. 2021). An increase in the voltage causes an increase in the electric current, increasing the temperature, which can in turn increase the solubility of $Al(OH)_3$ precipitates and the formation of unstable flocs. This decreases the electrocoagulation efficiency.

Weight Loss of Electrode and Sludge Generation

During the electrocoagulation process, several phenomena occur, including coagulant formation from anode oxidation, destabilization of contaminant particles, and particle aggregation for floc formation (Lakshmanan et al. 2009). The formation of larger flocs allowed solid particles to settle by gravity (Figs. S-3 and S-4) during the sedimentation process (Fig. S-3, f) and during the electrocoagulation process (Fig. S-3, e). Figure S-4 shows the electrocoagulation experiment with the Al electrode, 30 min contact time, and 2 A current, which was characterized by floc deposition 2 cm above the bottom of the reactor, whereas the floc thickness at the iron electrode was only 1 cm above the bottom of the reactor. The amount of coagulant agent formed affected the number of flocs formed and deposited at the bottom of the reactor. Larger currents and longer contact times tended to increase floc formation at the bottom of the reactor. This is because the production of Al^{3+} and Fe^{2+} ions from the electrode was sufficient to form the core of the floc. The flocs bound together to form larger flocs. In the coagulation-flocculation process, flocs with heavier masses form when coagulant chemicals or polymers are added. In the electrocoagulation process, the amount of Al and Fe dissolved in the electrode is proportional to the amount of current and contact time given to the system, in accordance with Faraday's Law 1 (Ciobanu et al. 2007). Thus, the greater the applied current and the longer the contact time, the more Al^{3+} and

Fe^{2+} ions are released from the anode and bind strongly to OH^-. The particles are destabilized and form flocs rapidly and in large quantities.

The flocs formed in the electrocoagulation process not only settled at the bottom of the reactor but also floated on the surface of the water. This occurred due to the formation of gas bubbles during the electrolysis process (Fig. 9), which pushed the particles to the surface (flotation). The bubbles were H_2 gas that formed at the cathode. The greater the current applied to the system, the faster the occurrence of hydrogen bubble production (Attour et al. 2014). The H_2 gas bubbles were small and varied in size from 15 to 80 µm and served to move pollutant particles to the liquid surface (Murugananthan et al. 2004). Electrolyte bubbles cause mixing in the solution through an upward momentum flux, thus increasing the effectiveness of the contact between the coagulant particles and pollutants (Holt 2002).

Conclusions

This study on electrocoagulation technology was conducted to remove colloidal clay from mine water with a relatively high TSS. The results showed that electrocoagulation using Al electrodes with a current of 2 A and contact time of 15 min had the greatest TSS removal efficiency (99%). For the Fe electrodes, the greatest TSS removal was achieved at a current of 2 A and contact time of 30 min, with a removal efficiency of 98%. The electrode type, current, and contact time are important factors in the effectiveness of colloidal clay removal. The Al electrodes performed better in removing the TSS than the Fe electrodes. In theory, the effectiveness of the Al electrodes can also be observed from the reactivity series of metals, which illustrates that Al is more reactive than Fe. The potential use of electrocoagulation technology for the removal of colloidal clay from mine water at a field scale exists, but several design criteria issues must be resolved, including cell geometry, reactor design, and cost analysis. Therefore, further research is necessary to identify the optimum design that can meet the challenges of scaling up in the field, including the use of continuous reactors and solar power in remote mining areas.

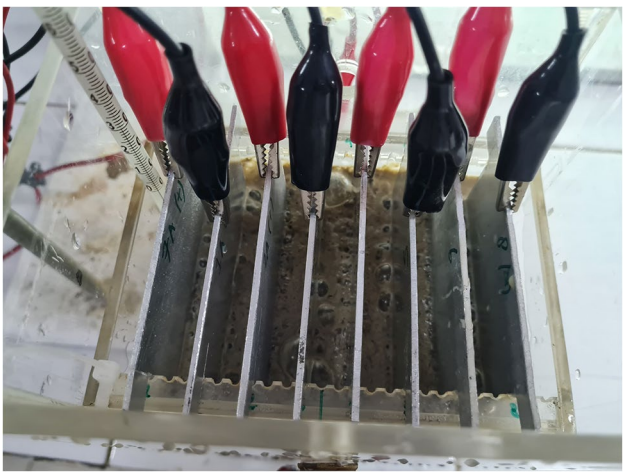

Fig. 9 Bubbles that cause flotation at the aluminum electrodes ($t_d = 15$ min, I = 2 A)

Supplementary Information The online version contains supplementary material available at https://doi.org/10.1007/s10230-024-01004-1.

Acknowledgements This study was supported by the Bandung Institute of Technology through the Water and Wastewater Engineering Research Group (KK-RALC) Faculty of Civil and Environmental Engineering research grant as part of the program titled 'Program Penelitian dan Pengabdian kepada Masyarakat (P2MI) ITB 2022.' The Environment Department of PT. Berau Coal, and PT. Ganeca Environmental Services provided financial and technical support for this study.

Data availability Data available within the article.

References

Abollino O, Giacomino A, Malandrino M, Mentasti E (2008) Interaction of metal ions with montmorillonite and vermiculite. Appl Clay Sci 38(3–4):227–236. https://doi.org/10.1016/j.clay.2007.04.002

Amri I, Meldha Z, Herman S, Karmila D, Fadilah Ramadani MhD, Nirwana (2023) Effects of electric voltage and number of aluminum electrodes on continuous electrocoagulation of liquid waste from the palm oil industry. Mater Today Proc 87:345–349. https://doi.org/10.1016/j.matpr.2023.03.621

APHA (2017) American public health association standard methods for the examination of water and wastewater, 23rd edn. American Public Health Association, Washington, DC

Arnita Y, Elystia S, Adesgur I (2017) Removal of cod and tss levels in batik dyeing wastewater using the electrocoagulation method. J Online Students Fac Eng Riau 4:1–9 (**in Indonesian**)

Attour A, Touati M, Tlili M, Ben Amor M, Lapicque F, Leclerc J-P (2014) Influence of operating parameters on phosphate removal from water by electrocoagulation using aluminum electrodes. Sep Purif Technol. https://doi.org/10.1016/j.seppur.2013.12.030

Bener S, Bulca Ö, Palas B, Tekin G, Atalay S, Ersöz G (2019) Electrocoagulation process for the treatment of real textile wastewater: effect of operative conditions on the organic carbon removal and kinetic study. Process Saf Environ Prot 129:47–54. https://doi.org/10.1016/j.psep.2019.06.010

Bergaya F, Theng BKG, Lagaly G (2006) Handbook of clay science. Elsevier, Amsterdam

Boinpally S, Kolla A, Kainthola J, Kodali R, Vemuri J (2023) A state-of-the-art review of the electrocoagulation technology for wastewater treatment. Water Cycle. https://doi.org/10.1016/j.watcyc.2023.01.001

Cao Y, Ma C, Yao J, Chen W, Gu L, Liu H, Liu C, Xiong J, Huangfu X (2022) Impact of biochar colloids on thallium(I) transport in water-saturated porous media: effects of pH and ionic strength. Chemosphere. https://doi.org/10.1016/j.chemosphere.2022.137152

Chen G (2004) Electrochemical technologies in wastewater treatment. Sep Purif Technol 38(1):11–41. https://doi.org/10.1016/j.seppur.2003.10.006

Chen C, Zhao K, Shang J, Liu C, Wang J, Yan Z, Liu K, Wu W (2018) Uranium (VI) transport in saturated heterogeneous media: influence of kaolinite and humic acid. Environ Pollut Uranium. https://doi.org/10.1016/j.envpol.2018.04.095

Chen L, Zhao Y, Bai H, Ai Z, Chen P, Hu Y, Song S, Komarneni S (2020) Role of montmorillonite, kaolinite, or illite in pyrite flotation: differences in clay behavior based on their structures. Langmuir 36:10860–10867. https://doi.org/10.1021/acs.langmuir.0c02073

Chen S, Xie J, Wen Z (2021) Chapter 4- Microalgae-based wastewater treatment and utilization of microalgae biomass. In: Li Y, Zhou W (eds) Advances in bioenergy. Elsevier, Amsterdam, pp 165–198. https://doi.org/10.1016/bs.aibe.2021.05.002

Ciobanu M, Wilburn JP, Krim ML, Cliffel DE (2007) Handbook of electrochemistry. Elsevier, Amsterdam. https://doi.org/10.1016/b978-0-444-51958-0.x5000-9

Dang PT, Dang VC (2018) Mine water treatment in Hongai coal mines. E3S Web Conf 35:01007. https://doi.org/10.1051/e3sconf/20183501007

Dogra SR, Dogra S (1990) Physical chemistry and questions. UI Press, Jakarta

Dos Anjos VE, Rohwedder JR, Cadore S, Abate G, Grassi MT (2014) Montmorillonite and vermiculite as solid phases for the preconcentration of trace elements in natural waters: adsorption and desorption studies of As, Ba, Cu, Cd Co, Cr, Mn, Ni, Pb, Sr, V, and Zn. Appl Clay Sci 99:289–296. https://doi.org/10.1016/j.clay.2014.07.013

Du S, Jin W, Qiao G, Fang H (2021) Study on the relationship between suspended solids concentration and turbidity in coal mine water. Res Square Platform LLC. https://doi.org/10.21203/rs.3.rs-442907/v1

Duan J, Gregory J (2003) Coagulation by hydrolysing metal salts. Adv Colloid Interface Sci 100–102:475–502. https://doi.org/10.1016/s0001-8686(02)00067-2

Ebba M, Asaithambi P, Alemayehu E (2021) Investigation on operating parameters and cost using an electrocoagulation process for wastewater treatment. Appl Water Sci 11:175. https://doi.org/10.1007/s13201-021-01517-y

El-Ashtoukhy E-SZ, Amin NK, Abdelwahab O (2009) Treatment of paper mill effluents in a batch-stirred electrochemical tank reactor. Chem Eng J 146(2):205–210. https://doi.org/10.1016/j.cej.2008.05.037

Ghernaout D, Ghernaout B (2012) Sweep flocculation as a second form of charge neutralisation—a review. Desalin Water Treat 44(1–3):15–28. https://doi.org/10.1080/19443994.2012.691699

Hamza A, Hussein IA, Mahmoud M (2023) Chapter 1- Introduction to reservoir fluids and rock properties. In: Hussein IA, Mahmoud M (eds) Developments in petroleum science. Elsevier, Amsterdam, pp 1–19. https://doi.org/10.1016/B978-0-323-99285-5.00003-X

Harahap MG, Abfertiawan MS, Syafila M (2024) Challenges in using electrocoagulation process in removal of Nickel metal in wastewater: a literature review. Inst Res Commun Serv Diponegoro Univ (LPPM UNDIP) 21(2):300–323https://doi.org/10.14710/presipitasi.v21i2

Hidayanti A, Afifa UI, Ismuyanto B, Juliananda J (2021) The effect of electrocoagulation voltage and dye initial concentration to the removal percentage of Rhemazol red RB. Rekayasa Bahan Alam dan Energi Berkelanjutan 5(2):1–9. https://doi.org/10.21776/ub.rbaet.2021.005.02.01. (**in Indonesian**)

Holt PK (2002) Electrocoagulation: unravelling and synthesising the mechanism behind a water treatment process. Thesis, Dept of Chemical Eng, Univ of Sydney, Sydney

Hudori (2008) Laundry wastewater treatment using electrocoagulation. Thesis, Bandung Institute of Technology (in Indonesian)

Kahr G, Madsen FT (1995) Determination of the cation exchange capacity and the surface area of bentonite, illite and kaolinite by methylene blue adsorption. Appl Clay Sci 9(5):327–336. https://doi.org/10.1016/0169-1317(94)00028-O

Karhu M, Kuokkanen V, Kuokkanen T, Rämö J (2012) Bench scale electrocoagulation studies of bio oil-in-water and synthetic oil-in-water emulsions. Sep Purif Technol. https://doi.org/10.1016/j.seppur.2012.06.003

Kleinmann B, Sobolewski A, Skousen J (2022) The evolving nature of active, passive, and semi-passive mine water treatment technology. In: Pope J, Wolkersdorfer C, Rait R, Trumm D, Christenson H, Wolkersdorfer C (eds), Proc, IMWA 2022 – Reconnect, pp 187–193. www.imwa.info/docs/imwa_2022/IMWA2022_Kleinmann_187.pdf

Koren JPF, Syversen U (1995) State-of-the-art electroflocculation. Filtr Separat 32(2):153–156. https://doi.org/10.1016/S0015-1882(97)84039-6

Kumar D, Sharma C (2022) Paper industry wastewater treatment by electrocoagulation and aspect of sludge management. J Cleaner Prod 360:131970. https://doi.org/10.1016/j.jclepro.2022.131970

Lagaly G (2006) Chapter 5- Colloid clay science. In: Bergaya F, Lagaly G (eds) Developments in clay science. Elsevier, Amsterdam, pp 141–245. https://doi.org/10.1016/s1572-4352(05)01005-6

Lakshmanan D, Clifford DA, Samanta G (2009) Ferrous and ferric ion generation during iron electrocoagulation. Environ Sci Technol 43(10):3853–3859. https://doi.org/10.1021/es8036669

Linares-Hernández I, Barrera-Díaz C, Roa-Morales G, Bilyeu B, Ureña-Núñez F (2009) Influence of the anodic material on electrocoagulation performance. Chem Eng J 148:97–105. https://doi.org/10.1016/j.cej.2008.08.007

Mamelkina MA, Cotillas S, Lacasa E, Sáez C, Tuunila R, Sillanpää M, Häkkinen A, Rodrigo MA (2017) Removal of sulfate from mining waters by electrocoagulation. Sep Purif Technol 182:87–93

Mao Y, Zhao Y, Cotterill S (2023) Examining current and future applications of electrocoagulation in wastewater treatment. Water 15(8):1455. https://doi.org/10.3390/w15081455

Marsh A, Heath A, Patureau P, Evernden M, Walker P (2018) Alkali activation behaviour of un-calcined montmorillonite and illite clay minerals. Appl Clay Sci. https://doi.org/10.1016/j.clay.2018.09.011

Matteson MJ, Dobson RL, Glenn RW Jr, Kukunoor NS, Waits WH III, Clayfield EJ (1995) Electrocoagulation and separation of aqueous suspensions of ultrafine particles. Colloids Surf A Physicochem Eng Aspects 104(1):101–109. https://doi.org/10.1016/0927-7757(95)03259-G

Mohapatra DP, Kirpalani DM (2017) Process effluents and mine tailings: sources, effects and management and role of nanotechnology. Nanotechnol Environ Eng 2:1. https://doi.org/10.1007/s41204-016-0011-6

Mollah MYA, Schennach R, Parga JR, Cocke DL (2001) Electrocoagulation (EC) – science and applications. J Hazard Mater 84:29–41. https://doi.org/10.1016/s0304-3894(01)00176-5

Mollah MY, Morkovsky P, Gomes JA, Kesmez M, Parga J, Cocke DL (2004) Fundamentals, present and future perspectives of electrocoagulation. J Hazard Mater 114:199–210. https://doi.org/10.1016/j.jhazmat.2004.08.009

Moneer AA, Thabet WM, Khedawy M, El-Sadaawy MM, Shaaban NA (2023) Electrocoagulation process for oily wastewater treatment and optimization using response surface methodology. Int J Environ Sci Technol. https://doi.org/10.1007/s13762-023-05003-7

Mouedhen G, Feki M, De Petris Wery M, Ayedi HF (2008) Behavior of aluminum electrodes in electrocoagulation process. J Hazard Mater 150(1):124–135. https://doi.org/10.1016/j.jhazmat.2007.04.090

Murugananthan M, Raju GB, Prabhakar S (2004) Removal of sulfide, sulfate and sulfite ions by electrocoagulation. J Hazard Mater 109(1–3):37–44. https://doi.org/10.1016/j.jhazmat.2003.12.009

Ni'am MF, Othman F, Sohaili J, Dan Fauzia Z (2007) Removal of COD and turbidity to improve wastewater quality using electrocoagulation technique. Malays J Anal Sci 11:198–205

Nur A, Effendi AJ (2014) Application of aluminum electrocoagulation electrodes in greywater recycling process at hotel. The institute for research and community services (LPPM) ITB. J Environ Eng 20(1):58–67. https://doi.org/10.5614/jtl.2014.20.1.7. (**in Indonesian**)

Oncel MS, Muhcu A, Demirbas E, Kobya M (2013) A comparative study of chemical precipitation and electrocoagulation for treatment of coal acid drainage wastewater. J Environ Chem Eng 1(4):989–995. https://doi.org/10.1016/j.jece.2013.08.008

Rodriguez J, Stopić S, Krause G, Friedrich B (2007) Feasibility assessment of electrocoagulation towards a new sustainable wastewater treatment. Environ Sci Pollut Res Int 14:477–482. https://doi.org/10.1065/espr2007.05.424

Sadik MA (2019) A review of promising electrocoagulation technology for the treatment of wastewater. Adv Chem Eng Sci 9(1):109–126. https://doi.org/10.4236/aces.2019.91009

Setyawati H, Galuh D, Yunita E (2021) Effect of electrode distance and voltage on CR, COD, and TSS reduction in industrial tannery wastewater using batch electrocoagulation. J Teknol Berkelanjutan Sains Terapan 2403:24–30 (**[in Indonesian]**)

Sillanpaa M, Shestakova M (2017) Electrochemical water treatment methods: fundamentals, methods and full scale applications. Butterworth-Heinemann, Oxford

Stylianou M, Montel E, Zissimos A, Christoforou I, Dermentzis K, Agapiou A (2022) Removal of toxic metals and anions from acid mine drainage (AMD) by electrocoagulation: The case of North Mathiatis open cast mine. Sustain Chem Pharm Elsevier BV 29:100737 https://doi.org/10.1016/j.scp.2022.100737

Syafila M, Abfertiawan MS, Handajani M, Hasan F, Oktaviani H, Arifianingsih NN (2023) Statistical analysis in selecting the best electrode between aluminum and iron in Tss removal using electrocoagulation. Indones J Urban Environ Technol. https://doi.org/10.25105/urbanenvirotech.v6i2.17835

Syaichurrozi I, Sarto S, Sediawan WB, Hidayat M (2020) Effect of current and initial pH on electrocoagulation in treating the distillery spent wash with very high pollutant content. Water 13(1):11. https://doi.org/10.3390/w13010011

Tiaiba M, Merzouk B, Amour A, Mazour M, Leclerc J-P, Lapicque F (2017) Influence of electrodes connection mode and type of current in electrocoagulation process on the removal of a textile dye. Desalin Water Treat. https://doi.org/10.5004/dwt.2017.20502

Trumm D (2010) Selection of active and passive treatment systems for AMD—Flow charts for New Zealand conditions. N Z J Geol Geophys 53(2–3):195–210. https://doi.org/10.1080/00288306.2010.500715

Vicente C, Silva JR, Santos AD, Silva JF, Mano JT, Castro LM (2023) Electrocoagulation treatment of furniture industry wastewater. Chemosphere. https://doi.org/10.1016/j.chemosphere.2023.138500

Vik EA, Carlson DA, Eikum AS, Gjessing ET (1984) Electrocoagulation of potable water. Water Res 18(11):1355–1360. https://doi.org/10.1016/0043-1354(84)90003-4

Wang X, Gao Y, Jiang X, Zhang Q, Liu W (2021) Analysis on the characteristics of water pollution caused by underground mining and research progress of treatment technology. Adv Civil Eng. https://doi.org/10.1155/2021/9984147

Węgrzyn A, Tsurtsumia A, Witkowski S, Freitas O, Figueiredo S, Cybińska J, Stawiński W (2022) Vermiculite as a potential functional additive for water treatment bioreactors inhibiting toxic action of heavy metal cations upsetting the microbial balance. J Hazard Mater. https://doi.org/10.1016/j.jhazmat.2022.128812

Weiss SF, Christensen ML, Jørgensen MK (2021) Mechanisms behind pH changes during electrocoagulation. AIChE J 67:e17384. https://doi.org/10.1002/aic.17384

Younger PL, Banwart SA, Hedin RS (2002) Active treatment of polluted mine waters. Mine water, environmental pollution, vol 5. Springer, Dordrecht, pp 271–309. https://doi.org/10.1007/978-94-010-0610-1_4

Zaroun MM, Yari A (2019) Designing an Electrochemical System for Efficient Removal of Chromium from Leachate by Electrocoagulation Using a Solar Panel as the Power Supply. Int J Electrochem Sci Elsevier BV 14(7):6337–6346https://doi.org/10.20964/2019.07.57